

RESEARCH

Open Access



Evaluation of antiplasmodial activity in silico and in vitro of *N*-acylhydrazone derivatives

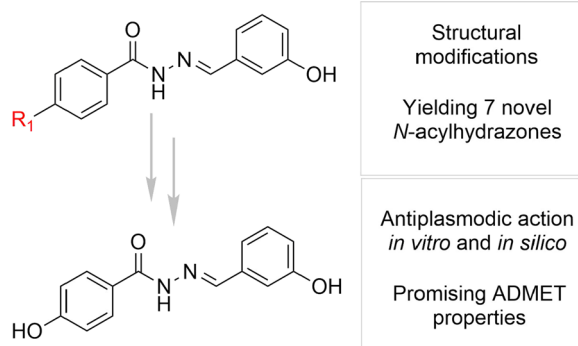
Fernanda A. Oliveira¹, Ana Claudia S. Pinto^{1*}, Caique L. Duarte¹, Alex G. Taranto¹, Eder Lorenzato Junior², Cleydson Finotti Cordeiro², Diogo T. Carvalho², Fernando P. Varotti¹ and Amanda L. Fonseca^{1*}

Abstract

N-acylhydrazones are considered privileged structures in medicinal chemistry, being part of antimicrobial compounds (for example). In this study we show the activity of *N*-acylhydrazone compounds, namely AH1, AH2, AH4, AH5 in in vitro tests against the chloroquine-resistant strain of *Plasmodium falciparum* (W2) and against WI26 VA-4 human cell lines. All compounds showed low cytotoxicity ($LC_{50} > 100 \mu\text{M}$). The AH5 compound was the most active against *Plasmodium falciparum*, with an IC_{50} value of $0.07 \mu\text{M}$. AH4 and AH5 were selected among the tested compounds for molecular docking calculations to elucidate possible targets involved in their mechanism of action and the SwissADME analysis to predict their pharmacokinetic profile. The AH5 compound showed affinity for 12 targets with low selectivity, while the AH4 compound had greater affinity for only one target (3PHC). These compounds met Lipinski's standards in the ADME in silico tests, indicating good bioavailability results. These results demonstrate that these *N*-acylhydrazone compounds are good candidates for future preclinical studies against malaria.

Keywords: Malaria, Bioinformatics, Molecular modeling

Graphical Abstract



Introduction

Malaria is an infectious disease caused by protozoa of the genus *Plasmodium* spp., and remains one of the major public health problems worldwide [1]. A total of 241 million cases and approximately 627,000 deaths were

*Correspondence: anaclsouza29@gmail.com; amalufonseca@gmail.com

¹ Núcleo de Pesquisa Em Química Biológica (NOBio), Universidade Federal de São João Del Rei, Campus Centro Oeste, Divinópolis, MG 35501-296, Brazil
Full list of author information is available at the end of the article



reported in 2020. The numbers represent a 6% increase in case reports compared to 2019 numbers. Increase associated with interruption of prevention and treatment during the COVID-19 pandemic, especially in Sub-Saharan Africa [2].

Five species are capable of infecting humans: *Plasmodium falciparum*, *Plasmodium vivax*, *Plasmodium ovale*, *Plasmodium malariae* and *Plasmodium knowlesi* [3]. The *P. vivax* and *P. falciparum* species are responsible for the majority of infections, with the latter being responsible for the largest number of deaths [4]. Correct identification of the infecting species is necessary to make an adequate therapeutic decision [5].

Malaria treatment consists of drugs based on natural products or synthetic compounds. Antimalarial drugs are delimited by class according to structural backbone and apparent action [4]. The following classes stand out: endoperoxides; 4-aminoquinolines; antifolates; naphthoquinones and 8-aminoquinolines [6]. With the emergence of multi-resistant strains in 2006, the World Health Organization (WHO) recommended changes to the treatment protocol for uncomplicated malaria caused by *P. falciparum*, and for malaria caused by chloroquine-resistant *P. vivax*, namely Artemisinin-based Combination Therapy (ACTs) [7].

The resistance to artemisinin in *P. falciparum* was first described in 2009 in Southeast Asia, mainly in the Greater Mekong region, a river which goes through some countries such as Cambodia and Vietnam [8]. Subsequently, the emergence of resistance was reported in African and South Asian countries [9].

Specific point mutations were identified in the k13 gene in artemisinin-resistant strains (Kelch13, PlasmoDB ID: PF3D7_1343700) [4]. The mutation of this gene causes the k13 protein to interfere in the role of the ubiquitination machinery, leading to a greater induction of protective stress responses caused by artemisinin, giving parasites a better adaptation in this environment [4, 9, 10].

The current therapeutic arsenal for malaria is limited and the emergence of in vitro and in vivo cases of resistance for ACTs makes the search for new options for compounds that can be used in clinical practice even more necessary [1, 11].

The *N*-acylhydrazone subunit is an important chemical group in drug discovery [12], as compounds with this structure have shown several biological applications, such as antiparasitic, antimicrobial, anticonvulsant [13], antiviral [14], analgesic, anti-inflammatory [15] and anti-proliferative action against tumor cells [16].

Melnyk and collaborators reported antiplasmodial activity of a library of acylhydrazones against *P. falciparum* chloroquine-resistant (W2) strain [17].

Küçükgülzel and collaborators described antiplasmodial activity of a series of acylhydrazones. The new compounds exhibited activity against chloroquine-resistant W2 and *P. falciparum* chloroquine-sensitive (3D7) strains [18].

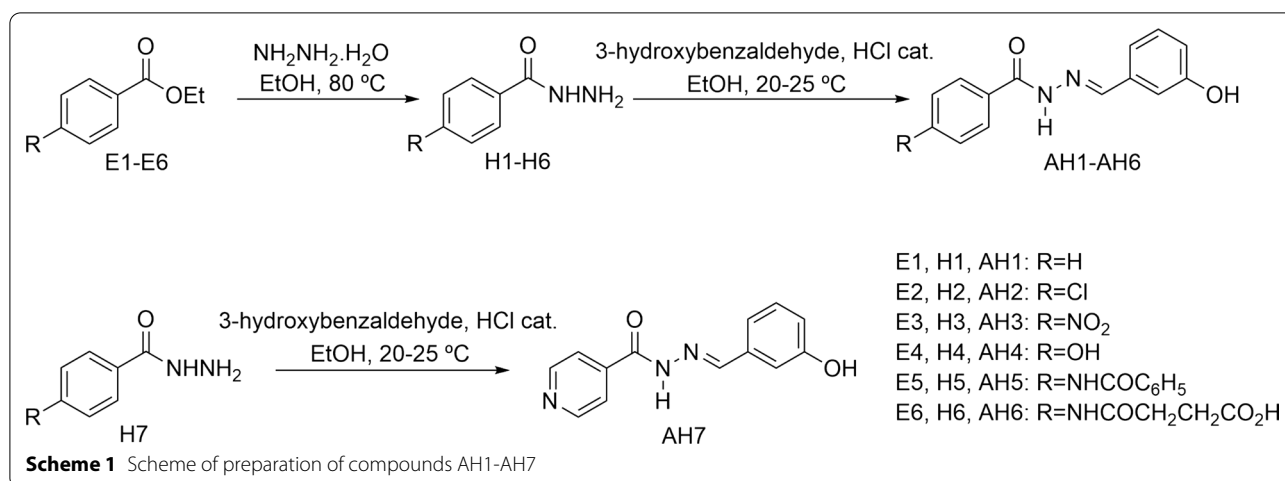
The process of developing new drugs consists of finding molecules capable of altering the function of a specific molecular target [19] to produce safer, more effective and accessible drugs [20]. An important data in order to ensure the activity of these new compounds is to study parameters like absorption, distribution, metabolism, excretion and toxicity (ADMET) during the process of development. These parameters are important to predict whether the compound is capable of becoming a bioactive molecule, which provides important data for the synthesis of possible drugs [21].

Another tool would be molecular docking, a tool that has been highlighted for its practicality, low cost and efficiency [22]. Fitting methods use a variety of algorithms to find the best pose of a ligand at the binding site, determining the main forces for molecular recognition and its affinity against a respective molecular target. This tool can therefore be useful to research and design more active ligands [23–25].

The use of in silico approaches has become increasingly frequent in malaria research, mainly as a tool that helps to describe the mechanism of action and reaction of antimalarials [26–30]. Knowledge about these mechanisms helps to predict possible unwanted interactions with other targets, in addition to guiding research aimed at structurally altering existing drugs, against which the parasite is already resistant in order to make them effective again [11, 31].

In order to understand the possible mechanism of action involved in using *N*-acylhydrazones as antimalarial compounds, one can simulate their interaction with a series of already described potential molecular targets deposited in data banks such as the Brazilian Malaria Molecular Targets (BraMMT) [11]. BraMMT is a molecular target bank created and validated by a research group which contains 35 pharmacological targets for *P. falciparum* [11].

Data banks like this enable performing inverse virtual screening (IVS), which is a process involving docking a single small-molecule, or a set of them, against a series of targets using previously validated docking software for these targets [32]. This process allows establishing an affinity relationship between the studied compounds and a specific target, comparing the binding energy generated with the binding energy of the crystallographic ligand, whose affinity has already been experimentally verified [33].



In view of the above, we report herein the synthesis, in silico properties and in vitro antiplasmodial activity of seven *N*-acylhydrazones.

Results and discussion

Chemistry

N-acylhydrazones (AH1-AH7) were prepared by a short synthesis route consisting in condensing the respective hydrazides H1-H7 with 3-hydroxybenzaldehyde as described previously with minor adaptations [34–38]. The hydrazides H1-H6 were obtained straightly by the hydrazinolysis of the esters E1-E6 [12–18]. The acylhydrazone HA6 is a new compound, while the others are already known substances. The overall synthesis is shown in Scheme 1.

The final products were obtained smoothly as crystalline solids in medium to high yields. The *N*-acylhydrazones were fully characterized by melting point, infrared (IR), nuclear magnetic resonance (NMR) and mass spectrometry (MS) analysis. First, the main findings in the IR spectra related to the acylhydrazones identities were the bands between 1670–1605 cm⁻¹, attributed to the *N*-acylhydrazone C=N and C=O groups. The analysis of the ¹H NMR spectra of AH1-AH7 showed a singlet around 8.3 ppm related to the iminic hydrogen (N=CH), which confirms the success in the condensation reaction. The same finding may be seen in ¹³C NMR spectra, where a signal in the range 146–148 ppm characteristic of the iminic carbon. All the other typical and expected signals for the final products were noted in the ¹H and ¹³C NMR spectra and their identities were further confirmed by the MS analysis.

In vitro activity of the *N*-acylhydrazones

The resistance of *Plasmodium* spp. to current drugs continues to grow and progressively limits the therapeutic

arsenal available for treating patients infected with malaria. Given the above, it is necessary to discover or design new pharmacologically active compounds [39].

N-acylhydrazone compounds stand out in medicinal chemistry because they have a large number of successful compounds that act on several molecular targets [40, 41]. These compounds are easily obtained by synthesis, since they are usually produced by a condensation reaction between aldehydes or ketones with hydrazides, and both the starting carbonyl reagent and hydrazides may have different structural frameworks [42]. Thus, they present themselves as an economically viable strategy for developing new libraries of chemical molecules [43, 44].

A set of criteria for validation of compounds are described in the development of new antimalarial drugs. The compounds to be tested in vitro should preferably comply with specific requirements: Lethal drug concentration that reduces parasite viability by 50% (IC₅₀) < 1 μM; minimum selectivity index (SI) values as 10, with the ideal being greater than 100 [11, 45].

The cytotoxicity test allows analyzing the survival rate of the cell line in the presence of the compounds. This identifies whether the compound is toxic or not to the cell line used [37]. To do so, the IC₅₀ was verified. The cytotoxicity presented against human lung fibroblast cell line WI-26VA4 (ATCC CCL-95.1) was comparable to that of chloroquine and artemether.

The in vitro tests were carried out with the purpose of evaluating antiplasmodial activity of the compounds synthesized against W2 strain. Chloroquine and artemether were used as a positive control and reference (Table 1).

The AH1, AH2, AH4, and AH5 compounds were active against W2 strain, and the IC₅₀ determined by the traditional test ranged from 0.07 to 2.15 μM. They did not demonstrate toxicity against WI-26VA4 cell line (LC₅₀ > 100 μM) (Table 1), comparable to that of

Table 1 In vitro antiplasmodial activity, cytotoxicity and selective index of *N*-acylhydrazone compounds AH1-AH7

Compounds	IC ₅₀ ± SD ^a (μM) ^b <i>P. falciparum</i>	LC ₅₀ ± SD ^a (μM) ^c WI-26VA4	SI ^d
AH1	0.19 ± 0.10	100 ± 0.25	526.31
AH2	2.15 ± 0.09	100 ± 0.33	46.51
AH3	Not determined	100 ± 0.19	Not determined
AH4	0.09 ± 0.05	100 ± 0.21	1,111.11
AH5	0.07 ± 0.07	100 ± 0.23	1,428.57
AH6	Not determined	100 ± 0.17	Not determined
AH7	Not determined	100 ± 0.13	Not determined
Chloroquine	0.057 ± 0.14	100 ± 0.22	1754.38
Artemether	< 1.01	100 ± 0.18	99.01

^a SD: Mean and standard deviation (SD) of triplicate experiments

^b 50% Inhibitory concentration against a *Plasmodium falciparum* chloroquine resistant (W2) strain

^c 50% Cytotoxic concentration against human lung fibroblast cell line (WI-26VA4)

^d Selectivity index (SI) = IC₅₀ (WI26VA4)/IC₅₀ (*P. falciparum*)

chloroquine and artemether, standard antimalarials. Compounds AH3, AH6 and AH7 were not active against the W2 strain, they had results greater than 1 μM, falling outside the established standard IC₅₀ < 1 μM [45]. Thus, in the table it was indicated as not determined. The SI was obtained through the relationship between the cytotoxic and antiplasmodic activity of each compound, making it possible to identify that the compounds are selective. These findings are in accordance with a set of criteria for the development of antimalarial drugs [45].

Among the in vitro results, the AH1, AH4 and AH5 compounds showed the best IC₅₀ values of 0.09 μM and 0.07 μM, respectively, and high SI of > 100. These findings corroborate the criteria for developing new antimalarial compounds announced in the literature [45].

Molecular docking

The binding energy is directly associated with the conformation adopted by the ligand inside the active site of the protein. Binding energy values lower than that of the crystallographic ligand are attributed to conformations that generate a more stable complex between the ligand of interest and the receptor. The evaluation of these energy values may suggest the most active compounds, as lower binding energy values suggest greater affinity between the compound and the tested target [25].

The energy values generated by the AutoDock Vina software program (Table 2—indexed at the end of the manuscript) demonstrated that the AH1 compound did not show the lowest binding, AH5 compound had the lowest binding energy values (between − 9.7 and − 0.3 kcal/mol) among the tested compounds for 23

targets. On the other hand, the AH4 compound had the lowest binding energy (between − 9.7 and − 8.7 kcal/mol) for 3 targets.

Among the targets in which the AH5 compound was the most active, it also obtained lower energy than the crystallographic ligand in only 12 of them. The AH4 compound had lower binding energy than the crystallographic one in only one of the targets in which it was the compound with the highest affinity. Due to the random character of the AutoDock Vina search algorithm, the results were performed in triplicate (Additional File 8: Data S1), suggesting that it is robust for virtual screening experiments.

The mechanism of action of acylhydrazones is still uncertain, and previous studies suggest that these compounds act by inhibiting malaria cysteine proteases, such as falcipain-2 [46]. However, analysis of the docking of our derivatives for falcipain-2 (represented in BraMMT by the target 3BPF) [47] showed that the most active compound for the target is AH6 (binding energy value of − 7.4 kcal/mol), which showed a high IC₅₀ in vitro.

The binding energy of the AH5 compound was less than that of the other compounds and that of the crystallographic ligand in the following proteins: 1NHW [48], 1O5X [49], 1QNG [50], 2PML [51], 3K7Y [52], 3T64 [53], 4B1B [54], 4C81 [55], 4N0Z [56], 4P7S [57], 4QOX [58], PFATP6 [59]. A possible explanation for this result is the presence of the benzene ring as the R substituent of the AH5 compound. The increase in non-polar groups in the molecule can cause a reduction in binding energy by up to − 1.0 kcal/mol per van der Waals bond, thus directly influencing the greater affinity of the compound; however, selectivity may vary depending on the presence of hydrophobic cavities in the region of the target's active site [61, 62].

The AH4 compound showed more affinity for only one target: 3PHC, having the lowest binding energy for that target with a binding energy of − 9.7 kcal/mol, compared to − 8.3 kcal/mol for the 3PHC crystallographic ligand, and it also showed an energy difference of − 1.7 kcal/mol for that target. Thus, an analysis of the interaction profile of the AH4 compound with the 3PHC target was made. The intermolecular interactions (Fig. 1) of the complex between the AH4 compound and the 3PHC target was generated by the Discovery Studio Visualizer software program.

The 3PHC target corresponds to *P. falciparum* purine phosphorylase (PfPNP) [63, 64]. This enzyme acts in the DNA synthesis pathway of the parasite through phosphorylating purines captured from the human erythrocyte. Studies using both inhibitory compounds, as well as genetic disruption, have shown that blocking PfPNP activity causes a defect in *P. falciparum* growth, mainly in

Table 2 Binding energy values of compounds *N*-acylhydrazone derivatives

Binding energy (kcal/mol)									
Target	AH1	AH2	AH3	AH4	AH5	AH6	AH7	Crystallographic ligand	Enzymatic class
1LF3	-6.6	-6.6	-6.7	7.0	-8.0	-7.7	-6.2	-9.6	Hydrolase
1LYX	-6.2	-5.6	-5.9	-6.3	-6.0	-7.6	-5.7	-5.6	Isomerase
1NHW	-7.3	-7.7	-7.7	-7.5	-9.1	-8.9	-7.1	-8.3	Oxidoreductase
1O5X	-5.1	-5.3	-5.5	-5.6	-6.3	-5.9	-5.1	-1.0	Isomerase
1QNG	-5.9	-6.0	-6.0	-6.2	-8.1	-7.6	-5.8	-7.7	Isomerase
1RL4	-6.1	-6.1	-6.1	-6.3	-6.8	-6.9	-5.8	-8.0	Hydrolase
1TV5	-9.2	-8.3	-8.1	-8.6	-7.1	-7.9	-7.9	-9.3	Oxidoreductase
1U4O	-6.2	-6.5	-7.0	-6.6	-7.4	-6.8	-6.2	-8.1	Oxidoreductase
1YWG	-7.0	-7.1	-7.3	-7.3	-7.6	-7.1	-6.7	-10.7	Oxidoreductase
2AAW	-6.2	-6.4	-6.2	-6.3	-7.0	-7.0	-5.7	-9.1	Transferase
2ANL	-6.9	-7.2	-7.3	-6.9	-7.8	-7.4	-6.6	-9.3	Hydrolase
2OK8	-4.7	-4.7	-5.3	-4.9	-5.6	-5.8	-4.6	-2.0	Oxidoreductase
2PML	-7.8	-8.1	-8.5	-8.1	-8.6	-8.6	-7.7	-6.9	Transferase
2Q8Z	-7.0	-6.8	-6.9	-7.6	-5.9	-5.3	-7.3	-9.7	Lyase
2VFA	-5.9	-5.9	-6.5	-5.9	-6.5	-6.6	-5.7	-1.0	Transferase
2VN1	-7.8	-8.0	-7.9	-7.7	-9.7	-9.2	-7.5	-14.6	Isomerase
2YOG	-8.5	-7.7	-7.8	-8.8	-8.9	-8.5	-7.8	-8.4	Lyase
3AZB	-0.2	-0.3	-0.3	-0.3	-0.3	-0.2	-0.3	-1.0	Hydrolase
3BPF	-6.3	-5.9	-6.2	-5.8	-7.0	-7.4	-5.8	-6.3	Signaling Protein
3CLV	-8.1	-8.2	-8.2	-8.0	-8.2	-8.7	-8.2	-11.7	Hydrolase
3FNU	-6.7	-7.1	-7.1	-6.8	-7.9	-7.9	-6.4	-9.2	Transferase
3K7Y	-7.5	-7.7	-7.4	-7.6	-8.5	-7.8	-7.4	-7.7	Lyase
3N3M	-7.4	-6.7	-8.0	-8.7	-5.7	-6.0	-7.8	-9.6	Transferase
3PHC	-9.4	-9.1	-8.6	-9.7	-8.2	-7.7	-8.8	-8.3	Hydrolase
3QS1	-7.5	-7.7	-7.2	-7.2	-9.0	-8.1	-6.7	-10.4	Hydrolase
3T64	-7.0	-7.4	-7.4	-7.0	-8.4	-7.8	-6.6	-8.1	Transferase
4B1B	-7.7	-7.4	-7.4	-7.9	-9.7	-9.1	-7.7	-12.3	Oxidoreductase
4C81	-5.6	-5.7	-5.6	-5.9	-6.9	-6.6	-5.5	-1.0	Lyase
4J56	-7.7	-7.6	-7.4	-7.9	-9.5	-9.5	-7.8	-13.0	Oxidoreductase
4N0Z	-5.5	-5.5	-5.4	-5.3	-6.1	-5.7	-5.3	-1.0	Oxidoreductase
4P7S	-5.7	-5.6	-6.0	-6.0	-6.9	-6.0	-5.4	-6.0	Cytokine Inhibitor
4QOX	-8.0	-8.1	-7.7	-7.8	-9.3	-8.3	-7.8	-8.9	Transferase
PfATP6	-7.8	-7.4	-7.4	-7.7	-8.4	-7.4	-7.4	-7.2	Transporter
PfHT	-7.3	-7.2	-7.5	-7.4	-8.4	-8.8	-7.2	-5.7	Transporter

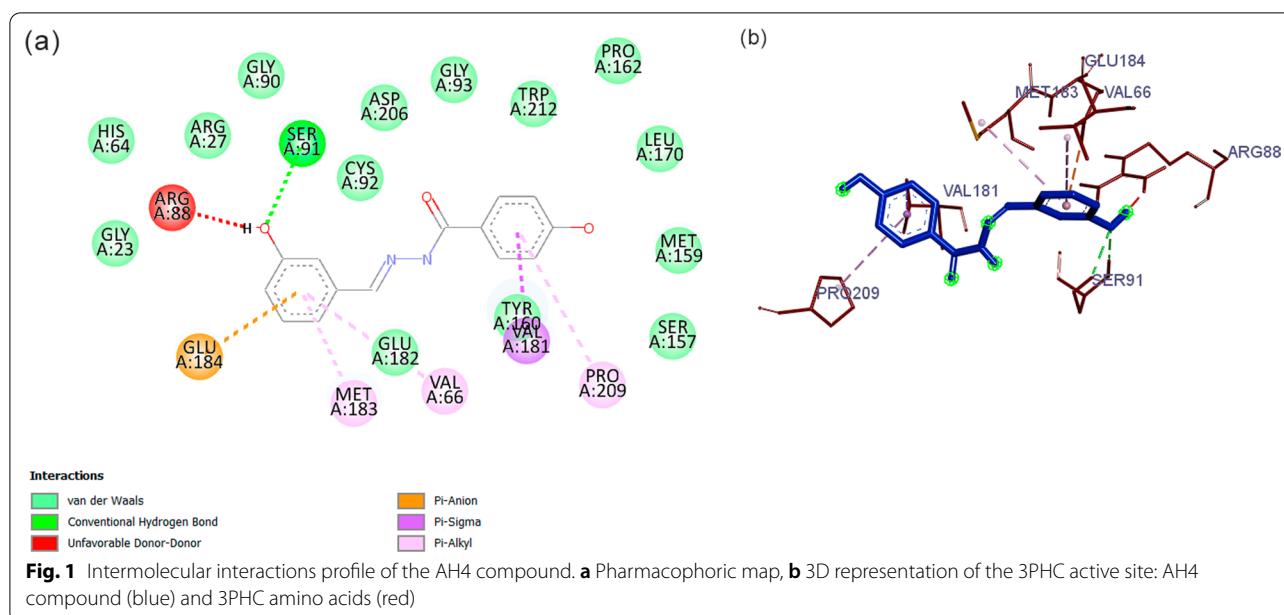
the trophozoite phase where the greatest activity of this enzyme as the protozoan replicates its genome and produces merozoites [63].

An analysis of the pharmacophoric map of the AH4 compound with PfPNP showed a hydrogen bond of the phenol group with a Ser96, in addition to interactions of the Pi-Anion and Pi-Alkyl type between Glu184, Val66 and Met183 and the phenolic ring. Other van der Waals interactions also occurred with a Pro209 and Val181. The phenolic group observed an unfavorable interaction with Arg88, which could negatively influence affinity.

Therefore, the set of other interactions attained proved to be compensatory. In view of this, more robust in silico studies, such as the use of molecular dynamics, are needed to assess the stability of the complex formed [64].

SwissADME

The oral administration route is the most recommended in developing drugs for tropical diseases, because it is considered easy for patients to adhere to treatment; therefore, it is necessary for the drugs to have good oral bioavailability they can be linked to good solubility and



essential permeability to predict the ability of compounds to reach their target at established concentrations [65, 66].

Ndombera concluded that an *in silico* analysis on the absorption, distribution, metabolism, excretion and toxicity of the compound (ADMET) can reduce failures related to pharmacokinetics in the clinical phase in drug development. Furthermore, it is a low cost *in silico* approach [67]. In view of the *in vitro* test, the AH4 and AH5 compounds which presented the best IC_{50} values of 0.09 μ M and 0.07 μ M, respectively, were evaluated under the ADMET parameters. Next, the AH3 compound, which presented the worst result in the *in vitro* test, and the standard chloroquine and artemether antimalarials were tested in the SwissADME software program (<http://www.swissadme.ch/>) to compare and validate the SwissADME study, shown in Table 3.

In this study, the criteria of the rule of five by Lipinski were evaluated, which aims to assess the similarity with a drug, the possibility of becoming an active oral medication and the physical–chemical properties [68]. To do so,

the compounds must be within the parameters: molecular weight (MW) less than 500 mg/dL, no more than 5 hydrogen bond donors (HD), no more than 10 hydrogen bond acceptors (HA), octanol-partition coefficient water (log P) not greater than 5 [21].

Other criteria were evaluated such as the polar topological surface area (TPSA) less than 140 Å, solubility in water (log S) having a value < -5 , the number of rotating connections (LR) less than < 9 [21]. The bioavailability score analyzed in the human colon carcinoma cell line in the value of 0.55 cm [21]. With these criteria within the established parameters, a compound with a good permeability to membranes is provided, indicating that the compound might have better absorption [69, 70].

Based on Table 3, compounds derived from *N*-acylhydrazones obtained results according to the Lipinski criteria, molecular weight 256.26–359.38 g/mol, number of hydrogen bond acceptors 2–5, number of hydrogen donors 0–3, clogP of 1.18–3.68. Lipophilicity is an important feature in the drug absorption and elimination process along with and a solubility in water which ranged

Table 3 SwissADME results of compounds derived from *N*-acylhydrazones

Compounds	MW < 500	HA < 10	HD < 5	Log P < 5	TPSA < 140 Å	Caco-2 (cm/s)	LR < 9	Log S > - 5
AH3	285.25	5	2	1.63	107.51	0.55	5	- 3.61
AH4	256.26	4	3	1.18	81.92	0.55	4	- 2.80
AH5	359.38	4	3	2.5	90.79	0.55	7	- 4.18
Chloroquine	305.85	2	1	3.68	28.16	0.56	8	- 4.21
Artemether	298.37	5	0	3.19	46.15	0.55	1	- 3.85

MW molecular weight, HA hydrogen bond acceptors, HD hydrogen bond donors, log P partition coefficient, TPSA polar topological surface area, Caco-2 Human Colon Carcinoma Cell Line, LR rotating bond, Log S solubility

from -2.80 to -4.18 mol/L, representing the compounds as soluble in water. The polar topological surface area (TPSA) values of the compounds did not exceed the parameters ranging from 28.16 – 107.51 Å, indicating that they will have significant permeability in the cell plasma membrane. Rotating connections (LR) ranged from 1 – 8 , not causing a negative effect on the permeation rate. The bioavailability score ranged between 0.55 – 0.56 cm, which means good pharmacokinetic property [71, 72].

Nugraha has demonstrated the importance of *in silico* evaluation using the SwissADME software program (<http://www.swissadme.ch/>) in order to analyze the efficacy of test compounds in predicting the pharmacokinetic properties for oral administration [73].

The results for the AH3, AH4, AH5 compounds and test compounds revealed that the compounds did not violate any of the standards established by ADMET, so they can be administered orally [21, 68–70]. Furthermore, correlating the results obtained *in vitro* with *in silico*, the AH4 compound showed agreement with the standards to be formulated as a good promising compound [68].

Conclusion

Considering the *in vitro* methods for evaluating the antiplasmodic and cytotoxic activity and *in silico* molecular modeling. The AH1, AH2, AH4 and AH5 compounds showed interesting properties for the continuation of the study, although experimental tests still need to be carried out to confirm the proposed mechanism of action and determine the structure–activity relationship of the compounds. Compounds AH4 and AH5 are being evaluated in an *in vivo* test, data that will be complementary to the *in silico* data presented.

Experimental

Chemistry

General methods

All reagents and solvents were purchased from Sigma (São Paulo, Brazil) and were used as such, except for the E1–E6 esters which were part of a household collection (Additional File 8: Data S1). The reaction courses were monitored by thin-layer chromatography (TLC) on silica gel G plates (Macherey–Nagel, DC-Fertigfolien ALUGRAM® XtraSil G/UV254) and different mixtures of hexanes/ethyl acetate as the eluents. Column grade silica gel (Sorbiline; 0.040 – 0.063 mm mesh size) was employed for column chromatography. Melting points of the compounds were obtained on a Bücher 535 melting-point apparatus and are uncorrected. Infrared (IR) spectra were recorded on a Shimadzu FTIR-Affinity-1. Nuclear Magnetic Resonance (NMR) spectra were recorded on a Bruker DPX 200 spectrometer (Rheinstetten, Germany) (200 MHz for ^1H NMR and 50 MHz for

^{13}C NMR spectra) in deuterated dimethylsulfoxide (DMSO- d_6). Chemical shifts (δ) were reported in parts per million (ppm) with reference to tetramethylsilane (TMS) as internal standard and coupling constants (J) were reported in Hertz (Hz). The LC–MS analysis were performed on an Acquity UPLC–H class system from Waters comprised of quaternary solvent manager attached to a triple-quadrupole (Acquity TQD) mass spectrometer. The output signals were monitored and processed using the Empower 3 software program. The samples were prepared in acetonitrile. Water spiked with 1% with trifluoroacetic acid and acetonitrile at the ratio 1:99 (v/v) was used as mobile phase. High-resolution mass spectrometry (HRMS) was recorded using an ESI micrOTOF–QII Bruker mass spectrometer.

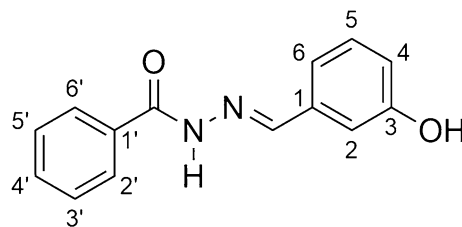
General method for the synthesis of hydrazides H1–H6

The respective ester (1 eq) and hydrazine hydrate 80% (5 eq) were stirred in ethanol (25 mL) under reflux for 8–48 h. Then, the reaction mixtures were cooled to 20 – 25 °C and then kept at 2 – 8 °C for 24 h. The solid hydrazides were collected by vacuum filtration, purified by recrystallization in hot ethanol and used as such for the next reactions. The identities of the hydrazides were confirmed by comparison of their IR and NMR spectra to the literature data and were in full agreement [34–38, 74].

General method for the synthesis of acylhydrazones AH1–AH7

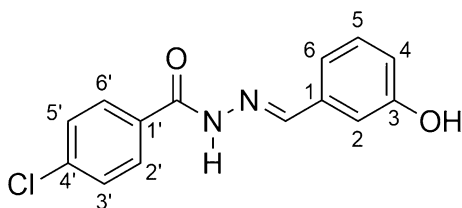
The respective hydrazide (1 eq), 3-hydroxybenzaldehyde (1 eq) and concentrated HCl (2 drops) were stirred in ethanol (20 mL) at 20 – 25 °C for 8 h. The acylhydrazones were obtained as crystalline solids after vacuum filtration and recrystallization with hot ethanol.

N'-[(1*E*)-(3-hydroxyphenyl)methylene]benzohydrazide (AH1, $\text{C}_{14}\text{H}_{12}\text{N}_2\text{O}_2$):



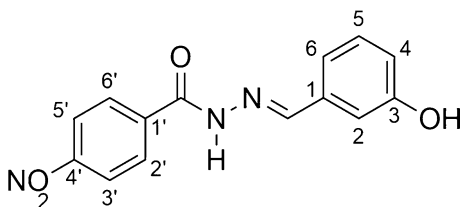
Yellowish solid; yield 91%; melting point: 195 – 196 °C. ^1H NMR (200 MHz, DMSO- d_6) δ 11.78 (s, 1H, NH), 9.61 (s, 1H, OH), 8.37 (s, 1H, N=CH), 7.91 (d, 2H, H-2' and H-6', $J = 5.6$ Hz), 7.61–7.50 (m, 3H, H-3', H-4', H-5'), 7.27–6.82 (m, 4H, H-2, H-4, H-5 and H-6); ^{13}C NMR (50 MHz, DMSO- d_6) δ 163.5 (C=O), 158.1 (C-3),

148.3 (N=CH), 136.0 (C-1), 133.9 (C-1'), 132.1 (C-4'), 130.3 (C-5), 128.9 (C-3' and C-5'), 128.0 (C-2' and C-6'), 119.2 (C-6), 117.9 (C-4), 113.0 (C-2). *4-chloro-N'-[(1E)-(3-hydroxyphenyl)methylene]benzohydrazide (AH2, C₁₄H₁₁ClN₂O₂)*:



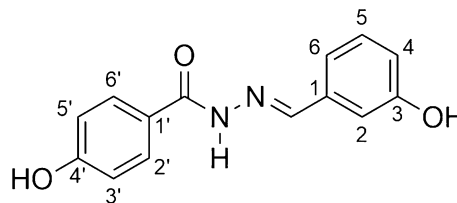
White solid; yield 85%; melting point: 221–223 °C. IR (ATR) $\bar{\nu}_{\text{max}}/\text{cm}^{-1}$: 3277 (v N–H), 3099 (v C–H ar), 1647 (v C=O), 1560 (v C=N), 1275 (v C–O); ¹H NMR (200 MHz, DMSO-d₆) δ 11.82 (s, 1H, NH), 9.59 (s, 1H, OH), 8.34 (s, 1H, N=CH), 7.91 (d, 2H, H_{2'} and H-6'; J=6.12 Hz), 7.58 (d, 2H, H-3' and H-5'; J=6.12 Hz), 7.23–6.80 (m, 4H, H₂, H-4, H-5 and H-6); ¹³C NMR (50 MHz, DMSO-d₆) δ 161.4 (C=O), 157.1 (C-3), 147.6 (N=CH), 136.0 (C-1), 134.9 (C-4'), 131.6 (C-1'), 129.3 (C-5), 129.0 (C-2' and C6'), 128.0 (C-3' and C-5'), 118.3 (C-6), 117.0 (C-4), 112.1 (C-2). MS (ESI) m/z calcd for C₁₄H₁₁ClN₂O₂ (M+H)⁺: 275.05, found 274.96.

N'-[(1E)-(3-hydroxyphenyl)methylene]-4-nitrobenzohydrazide (AH3, C₁₄H₁₁N₃O₄):



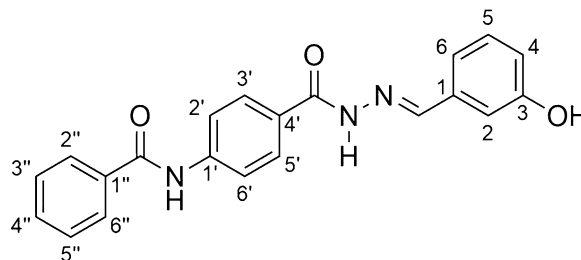
Light gray solid; yield 86%; melting point: 255–256 °C. IR (ATR) $\bar{\nu}_{\text{max}}/\text{cm}^{-1}$: 3280 (v NH), 3051 (v C–H ar), 1661 (v C=O), 1605 (v C=C ar), 1560 (v C=N), 1518 (v NO₂), 1348,2 (v NO₂), 1282 (v C–O); ¹H NMR (200 MHz, DMSO-d₆) δ 12.04 (s, 1H, NH), 9.61 (s, 1H, OH), 8.36 (s, 1H, N=CH), 8.34 (d, 2H, H-3' and H-5'; J=6.3 Hz), 8.13 (d, 2H, H-2' and H-6'; J=6.3 Hz), 7.26 (m, 4H, H-2, H-4, H-5 and H-6); ¹³C NMR (50 MHz, DMSO-d₆) δ 161.5 (C=O), 156.7 (C-3), 150.5 (C-4'), 139.5 (C-1'), 135.7 (C-1), 130.9 (C-2' and C-6'), 129.6 (C-5), 124.6 (C-3' and C-5'), 120.1 (C-6), 118.2 (C-4), 113.6 (C-2). MS (ESI) m/z calcd for C₁₄H₁₁N₃O₄ (M+H)⁺: 286.07, found 286.00.

4-hydroxy-N'-[(1E)-(3-hydroxyphenyl)methylene]benzohydrazide (AH4, C₁₄H₁₂N₃O₃):



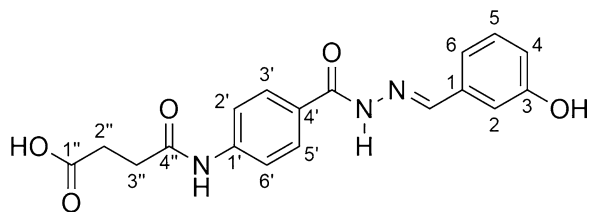
Light brown solid; yield 72%; melting point: 255–258 °C. IR (ATR) $\bar{\nu}_{\text{max}}/\text{cm}^{-1}$: 3200 (v N–H), 3051 (v C–H ar), 1619 (v C=O), 1585 (v C=N), 1236 (v C–O); ¹H NMR (200 MHz, DMSO-d₆) δ 11.61 (NH), 10.22 (OH), 9.69 (OH), 8.31 (N=CH), 7,79 (d, 2H, H_{2'} and C-6'; J=8.5 Hz); ¹³C NMR (50 MHz, DMSO-d₆) δ 164.5 (C=O), 162.3 (C-4'), 159.8 (C-3'), 147.9 (N=C), 137.4 (C-1), 132.1 (C-5), 131.4 (C-2' and C-6'), 125.5 (C1'), 121.8 (C-6), 119.6 (C-3' and C-5'), 116.7 (C-4), 114.3 (C-2). MS (ESI) m/z calcd for C₁₄H₁₂N₃O₃ (M+H)⁺: 257.08, found 256.99.

N-(4-[(2E)-2-(3-hydroxybenzylidene)hydrazino]carbonyl]phenyl) benzamide (AH5, C₂₁H₁₇N₃O₃):



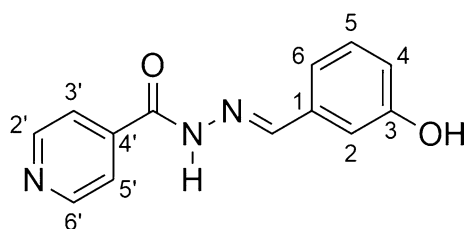
Light gray solid; yield 91%; melting point: 284–286 °C. IR (ATR) $\bar{\nu}_{\text{max}}/\text{cm}^{-1}$: 3423 (v O–H), 3319 (v N–H), 3242 (v N–H), 3079 (v C–H ar), 1651 (v C=O amide), 1633 (v C=O hydrazone), 1511 (v C=N), 1296 (v C–O); ¹H NMR (200 MHz, DMSO-d₆) δ 11.77 (s, 1H, CONHN=C), 10.54 (s, 1H, OH), 9.66 (s, 1H, CONHAr), 8.38 (s, 1H, N=CH), 8.00–6.82 (m, 13H, Harom); ¹³C NMR (50 MHz, DMSO-d₆) δ 166.2 (C=O), 162.9 (C=O), 158.0 (C-3), 147.8 (N=C), 142.7 (C-1'), 136.0 (C-1), 135.0 (C-1''), 132.2 (C-4''), 130.2 (C-3' and C-5'), 128.8 (C-3'' and C-5''), 128.4 (C-4'), 128.1 (C-2'' and C-6''), 119.8 (C-2' and C-6'), 119.1 (C-6), 117.7 (C-4), 112.9 (C-2). MS (ESI) m/z calcd for C₂₁H₁₇N₃O₃ (M+H)⁺: 360.13, found 360.06.

4-[(4-[(2E)-2-(3-hydroxybenzylidene)hydrazino]carbonyl]phenyl)amino]-4-oxobutanoic acid (AH6, C₁₈H₁₇N₃O₅):



Light gray solid; yield 65%; melting point: 232–234 °C. IR (ATR) $\bar{\nu}_{\text{max}}/\text{cm}^{-1}$: 3400–2400 (v O–H carboxylic acid), 3322 (v N–H), 3242 (v N–H), 3051 (v C–H ar), 1706 (v C=O carboxylic acid), 1665 (v C=O amide), 1644 (v C=O hydrazone), 1522 (v C=N), 1181 (v C–O); ¹H NMR (200 MHz, DMSO-d₆) δ 12.10 (s, 1H, COOH), 11.66 (CONHAr); 10.22 (CONHN=C), 9.59 (s, 1H, ArOH), 8.33 (N=CH), 7.85 (d, 2H, H-2' and H-6'; J=8.5 Hz), 7.69 (d, 2H, H-3' and H-5'; J=8.5 Hz), 7.25–6.78 (m, 4H, H-2, H-4, H-5 and H-6); 2.58–2.44 (m, 4H, H-2'', H-3''); ¹³C NMR (50 MHz, DMSO-d₆) δ 173.3 (C-4''), 170.1 (C-1''), 161.9 (CONHN), 157.1 (C-3), 146.9 (N=C), 141.8 (C-1'), 135.2 (C-1), 129.3 (C-3' and C-5'), 128.0 (C-5), 126.9 (C-4'), 118.2 (C-6), 117.6 (C-2' and C-6'), 116.8 (C-4), 112.0 (C-2), 30.64 (C-2''), 28.17 (C-3''). MS (ESI) m/z calcd for C₁₈H₁₇N₃O₅ (M+H)⁺: 356.12, found 356.01.

N'-[(1E)-(3-hydroxyphenyl)methylene]isonicotinohydrazide (AH7, C₁₃H₁₁N₃O₂):



Yellowish solid; yield 93%; melting point: 268–269 °C. IR (ATR) $\bar{\nu}_{\text{max}}/\text{cm}^{-1}$: 3474 (v OH), 3397 (v N–H), 3099 (v C–H ar), 1668 (v C=O), 1561 (v C=N), 1287 (v C–O); ¹H NMR (200 MHz, DMSO-d₆) δ 12.69 (s, 1H, NH), 9.04 (s, 1H, OH), 9.03 (d, 2H, H-2', H-6'; J=9.63 Hz), 8.54 (s, 1H, N=CH), 8.36 (d, 2H, H-3'; H-5'; J=9.63 Hz), 7.30–6.78 (m, 5H, H-2, H-4, H-5, H-6, OH); ¹³C NMR (50 MHz, DMSO-d₆) δ 159.9 (C=O), 154.7 (C-3), 150.4 (C-2' and C-6'), 146.2 (N=C), 145.3 (C-4'), 136.1 (C-1), 129.3 (C-5), 123.8 (C-3' and C-5'),

119.2 (C-6), 118.1 (C-4), 113.0 (C-2). MS (ESI) m/z calcd for C₁₃H₁₁N₃O₂ (M+H)⁺: 242.09, found 241.98.

Characterization of all compounds was presented in Additional File 8: Data.

In vitro activity of *N*-acylhydrazones

P. falciparum W2 strain were maintained in continuous culture using human red blood cells in RPMI 1640 medium, supplemented with human plasma [75]. The parasites were synchronized using sorbitol [76] treatment and the parasitemia was microscopically evaluated with Giemsa-stained blood smears.

The blood suspension was adjusted to 2% parasitemia and hematocrit, thus distributed into 96-wells of a microplate containing the *N*-acylhydrazones (AH1, AH2, AH3, AH4, AH5, AH6, AH7), artemether and chloroquine, standard anti-malarial in triplicate for each dose (Additional Files 1, 2, 3, 4, 5, 6, 7). After 48 h, blood smears were prepared, coded, stained with giemsa and examined at 1000× magnification [77]. The parasitemia of controls (considered as 100% growth) was compared to test cultures, and then the percentage of infected red blood cells was calculated.

The results were expressed as mean of half-maximal inhibitory dose (IC₅₀), with different drug concentrations performed in triplicate and compared with drug-free controls. Curve fitting was performed using OriginPro® 8.0 software (Origin Lab Corporation, Northampton, MA, USA).

Cytotoxicity test

Non-cancerous human lung fibroblast WI-26VA4 (ATC CCCL-95.1) cell line was used to assess the cell viability after each chemical treatment by employing the MTT colorimetric assay [78, 79]. First, 1 × 10⁶ cells were seeded in 96-well microplates with RPMI 1640, the medium supplemented was composed with fetal bovine serum (FBS) and Penicillin Streptomycin antibiotics. Next, microplates were incubated overnight at 37 °C and 5% CO₂, followed by treatment with *N*-acylhydrazone (AH1, AH2, AH3, AH4, AH5, AH6, AH7), artemether and chloroquine, solubilized in 0.1% DMSO (v/v). Negative controls were composed of cells without treatment. Five serial dilutions (1:10) were made from a stock solution (10 mg mL⁻¹) using RPMI supplemented with 1% FBS. Cell viability was evaluated after 48 h of incubation by discarding the medium and adding 100 μ L of 5% MTT, followed by 3 h of incubation. Then, the supernatant was discarded, and insoluble formazan product was dissolved in DMSO. The optical density (OD) of each well was measured using a microplate spectrophotometer at

550 nm. The OD of untreated control cells was defined as 100% cell viability and all assays were performed in triplicate. The selectivity index (SI) of samples was calculated by following Eq. 1 [29].

$$SI = \frac{LC_{50} \text{ of WI-26VA4 cell line}}{LC_{50} \text{ of } P. \textit{falciparum} \text{ (strain W2)}} \quad (1)$$

Equation 1 Selectivity index formula.

Molecular docking

Initially, the structure of the compounds was designed using the Marvin Sketch software program [80]. In this step, protonated form and tautomeric conformers were carefully checked using of hydrogen potential (pH) 7.4 and pH 4.0 [81]. Afterwards, all ligands were refined by semi-empirical Parametric Method 7 (PM7) [82] implemented on MOPAC2012 using the keyword ef for minimum search [83]. Next, refined ligands in pdbqt format were assigned rotatable bonds, Gasteiger–Marsili net atomic charges [84], and hydrogens from polar atoms were kept by the MGLTools software program [85]. The visual inspection of ligands geometry was performed using the Discovery Studio Visualizer software program [86].

After the ligands were prepared, two series of molecular docking calculations were performed using the AutoDock Vina software program (The Scripps Research Institute, La Jolla, CA) [87], coupled to the Octopus platform [88], one with the adjustment of the protonation state of the compounds to pH 7.4, consistent with the pH of the enzymatic environment of most targets, and the other with adjustment to pH 4.0, for the targets 1LF3 [89], 2ANL [90], 3BPF [91], 3FNU [92], 3QS1 [93], which are located in the digestive vacuole of the parasite.

Next, the binding energy generated during molecular docking for each compound was used to evaluate the results. Then, a comparison was made with the energy of the crystallographic ligands of each of the targets. The acylhydrazone derivatives that showed lower energy values in relation to the crystallographic ligand were classified as more active in *in silico* methods [25].

SwissADME

The synthetic derivatives of acylhydrazone were designed using Chem Axons Marvin JS (<http://www.chemaxon.com>), the structures of the compounds were used in the SwissADME software program (<http://www.swissadme.ch/>) of the Institute of bioinformatics (<http://www.sib.swiss>) to analyze the profile of the compounds, as well as their results of physical–chemical and pharmacokinetic parameters, and their similarity with drugs were examined [21, 38].

Abbreviations

ACTs: Artemisinin-based Combination Therapy; ADMET: Parameters of absorption, distribution, metabolism, excretion and toxicity; Arg: Arginine; BraMMT: Brazilian Malaria Molecular Targets; Caco-2: Human Colon Carcinoma Cell Line; DMSO: Dimethylsulfoxide; DMSO-d6: Deuterated dimethylsulfoxide; ESI: Electrospray ionization; FBS: Fetal bovine serum; Glu: Glutamate; HA: Hydrogen bond acceptors; HD: Hydrogen bond donors; Hz: Hertz; IC₅₀: Half-maximal inhibitory dose; IR: Infrared; IVS: Inverse virtual screening; J: Coupling constant; LC₅₀: Lethal drug concentration that reduced WI-26VA4 cells viability in 50%; log P: Partition coefficient; Log S: Solubility; LR: Rotating bond; Met: Methionine; MS: Mass spectrometry; MW: Molecular weight; NMR: Nuclear magnetic resonance; OD: Optical density; PDB: Protein data bank; PFPNP: *P. falciparum* Purine nucleoside phosphorylase; pH: Hydrogen potential; PM7: Parametric Method 7; ppm: Parts per million; Pro: Proline; RPMI: Growth medium used in culture; Ser: Serine; SD: Standard deviation; SI: Selectivity index; TLC: Thin-layer chromatography; TMS: Tetramethylsilane; TPSA: Polar topological surface area; TQD: Triple-quadrupole; UPLC-H: Acquity UPLC-H class system from Waters; Val: Valine; WI-26VA4: Human pulmonary fibroblast cells; W2: Chloroquine-resistant; WHO: World Health Organization; 3D7: *Plasmodium falciparum* Chloroquine-sensitive; δ: Chemical shifts.

Supplementary Information

The online version contains supplementary material available at <https://doi.org/10.1186/s13065-022-00843-9>.

Additional file 1: Figure SAH1. N-acylhydrazone compounds AH1.

Additional file 2: Figure SAH2. N-acylhydrazone compounds AH2.

Additional file 3: Figure SAH3. N-acylhydrazone compounds AH3.

Additional file 4: Figure SAH4. N-acylhydrazone compounds AH4.

Additional file 5: Figure SAH5. N-acylhydrazone compounds AH5.

Additional file 6: Figure SAH6. N-acylhydrazone compounds AH6.

Additional file 7: Figure SAH7. N-acylhydrazone compounds AH7.

Additional file 8: Data S1: Figures, IR, NMR and MS spectra for AH1–AH7 acylhydrazones

Acknowledgements

This study was financed by the Coordenação de Aperfeiçoamento de Pessoal de Nível Superior—Brasil (CAPES)—Finance Code 001, Brazilian National Council for Scientific and Technological Development (CNPq) process 310108/2020-9 and 303680/2021-0, and Fundação de Amparo à Pesquisa do Estado de Minas Gerais—Brasil (FAPEMIG).

Author contributions

ALF e CLD was responsible for the *in silico* tests; ACSP, ALF and FAO were responsible for *in vitro* tests; CFC, ELJ and DTC were responsible for the synthesis of compounds; ALF, AGT and FPV coordinated the study. All authors read and approved the final manuscript.

Funding

Coordenação de Aperfeiçoamento de Pessoal de Nível Superior—Brasil (CAPES), Finance Code 001 and postdoctoral fellowship, Finance Code 001 and postdoctoral fellowship, Finance Code 001 and postdoctoral fellowship, Finance Code 001 and postdoctoral fellowship, Finance Code 001 and postdoctoral fellowship, Finance Code 001 and postdoctoral fellowship, Universidade Federal de São João del-Rei—Campus Centro-Oeste Dona Lindu (CCO), Conselho Nacional de Desenvolvimento Científico e Tecnológico—Brasil (CNPq), 310108/2020-9, 310108/2020-9, Fundação de Amparo à Pesquisa do Estado de Minas Gerais—Brasil (FAPEMIG), APQ-02742-17, APQ-02742-17, Universidade Federal de Alfenas

Availability of data and materials

All data generated or analyzed during this study are included in this published article [and its supplementary information files].

Declarations

Ethics approval and consent to participate

Not applicable.

Consent for publication

All authors read and approved the final manuscript.

Competing interests

The authors declare that they have no competing interests.

Author details

¹Núcleo de Pesquisa Em Química Biológica (NQBio), Universidade Federal de São João Del Rei, Campus Centro Oeste, Divinópolis, MG 35501-296, Brazil.

²Laboratório de Pesquisa Em Química Farmacêutica, Universidade Federal de Alfenas, Campus Alfenas, Alfenas, MG 37130-001, Brazil.

Received: 25 March 2022 Accepted: 17 June 2022

Published online: 09 July 2022

References

- Araújo RV, Santos SS, Sanches LM, Giarolla J, El Seoud O, Ferreira EI. Malaria and tuberculosis as diseases of neglected populations: state of the art in chemotherapy and advances in the search for new drugs. Mem Inst Oswaldo Cruz. 2020. <https://doi.org/10.1590/0074-02760200229>.
- WHO (2021). World Malaria Report 2021, Switzerland: World Health Organization. Available from: <https://www.who.int/publications/i/item/9789240040496>. Accessed 15 May 2022.
- Phillips MA, Burrows JN, Manyando C, van Huijsduijnen RH, Van Voorhis WC, Wells TNC. Malaria. Nat Rev Dis Prim. 2017. <https://doi.org/10.1038/nrdp.2017.50>.
- Ross LS, Fidock DA. Elucidating mechanisms of drug-resistant *Plasmodium falciparum*. Cell Host Microbe. 2019. <https://doi.org/10.1016/j.chom.2019.06.001>.
- Kotepui M, Kotepui KU, De Jesus Milanez G, Masangkay FR. *Plasmodium* spp. mixed infection leading to severe malaria: a systematic review and meta-analysis. Sci Rep. 2020. <https://doi.org/10.1038/s41598-020-68082-3>.
- Sato S. *Plasmodium*—a brief introduction to the parasites causing human malaria and their basic biology. J Physiol Anthropol. 2021. <https://doi.org/10.1186/s40101-020-00251-9>.
- Gething PW, Casey DC, Weiss DJ, Bisanzio D, Bhatt S, Cameron E, et al. Mapping *Plasmodium falciparum* mortality in Africa between 1990 and 2015. N Engl J Med. 2016. <https://doi.org/10.1056/NEJMoa1606701>.
- Alam MS, Ley B, Nima MK, Johora FT, Hossain ME, Thriemer K, et al. Molecular analysis demonstrates high prevalence of chloroquine resistance but no evidence of artemisinin resistance in *Plasmodium falciparum* in the Chittagong Hill Tracts of Bangladesh. Malar J. 2017. <https://doi.org/10.1186/s12936-017-1995-5>.
- Tilley L, Straimer J, Gnädig NF, Ralph SA, Fidock DA. Artemisinin action and resistance in *Plasmodium falciparum*. Trends Parasitol. 2016. <https://doi.org/10.1016/j.pt.2016.05.010>.
- Bridgford JL, Xie SC, Cobbold SA, Pasaje CFA, Herrmann S, Yang T, et al. Artemisinin kills malaria parasites by damaging proteins and inhibiting the proteasome. Nat Commun. 2018. <https://doi.org/10.1038/s41467-018-06221-1>.
- Nunes RR, da Fonseca AL, Pinto ACDS, Maia EHB, da Silva AM, Varotti FDP, et al. Brazilian malaria molecular targets (BraMMT): selected receptors for virtual highthroughput screening experiments. Mem Inst Oswaldo Cruz. 2019. <https://doi.org/10.1590/0074-02760180465>.
- Cachiba TH, Carvalho BD, Carvalho DT, Cusinato M, Prado CG, Dias ALT. Síntese e avaliação preliminar da atividade antibacteriana e antifúngica de derivados *N*-acilidrazônicos. Quim Nova. 2012. <https://doi.org/10.1590/S0100-40422012000800014>.
- Küçüküzümlü SG, Mazi A, Sahin F, Öztürk S, Stables J. Synthesis and biological activities of diflunisal hydrazide-hydrazones. Eur J Med Chem. 2003. <https://doi.org/10.1016/j.ejmech.2003.08.004>.
- Savini L, Chiasserini L, Travagli V, Pellerano C, Novellino E, Cosentino S, et al. New α -(*N*)-heterocyclhydrazone: evaluation of anticancer, anti-HIV and antimicrobial activity. Eur J Med Chem. 2003;39:113–22.
- Barreiro EJ, Fraga CAM, Miranda ALP, Rodrigues CR. A química medicinal de *N*-acilidrazonas: novos compostos-protótipos de fármacos analgésicos, antiinflamatórios e anti-trombóticos. Quim Nova. 2002. <https://doi.org/10.1590/S0100-40422002000100022>.
- Vogel S, Kaufmann D, Pojarová M, Müller C, Pfaller T, Kühne S, et al. Aroyl hydrazones of 2-phenylindole-3-carbaldehydes as novel antimicrobial agents. Bioorg Med Chem. 2008;16:6436–47.
- Melnyk P, Leroux V, Sergheraert C, Grellier P. Design, synthesis and in vitro antimalarial activity of an acylhydrazone library. Bioorg Med Chem Lett. 2006. <https://doi.org/10.1016/j.bmcl.2005.09.058>.
- Rollas S, Küçüküzümlü S. Biological activities of hydrazone derivatives. Molecules. 2007. <https://doi.org/10.3390/12081910>.
- Knowles J, Gromo G. Target selection in drug discovery. Nat Rev Drug Discov. 2003. <https://doi.org/10.1038/nrd986>.
- Okombo J, Chibale K. Insights into integrated lead generation and target identification in malaria and tuberculosis drug discovery. Acc Chem Res. 2017. <https://doi.org/10.1021/acs.accounts.6b00631>.
- Daina A, Michielin O, Zoete V. SwissADME: a free web tool to evaluate pharmacokinetics, drug-likeness and medicinal chemistry friendliness of small molecules. Sci Rep. 2017. <https://doi.org/10.1038/srep42717>.
- Cavasotto CN, Acuar MG, Adler NS. Computational chemistry in drug lead discovery and design. Int J Quantum Chem. 2018. <https://doi.org/10.1002/qua.25678>.
- Kitchen DB, Decornez H, Furr JR, Bajorath J. Docking and scoring in virtual screening for drug discovery: methods and applications. Nat Rev Drug Discov. 2004. <https://doi.org/10.1038/nrd1549>.
- Chaudhary KK, Mishra N. A review on molecular docking: novel tool for drug discovery. JSM Chem. 2016;4:1029.
- Ferreira L, dos Santos R, Oliva G, Andricopulo A. Molecular docking and structure-based drug design strategies. Molecules. 2015. <https://doi.org/10.3390/moléculas200713384>.
- Prakash N. Molecular docking studies of antimalarial drugs for malaria. J Comput Sci Syst Biol. 2010. <https://doi.org/10.4172/jcsb.1000059>.
- Da FAL, Nunes RR, Braga VML, Comar M Jr, Alves RJ, Varotti FDP, et al. Docking, QM/MM, and molecular dynamics simulations of the hexose transporter from *Plasmodium falciparum* (PfHT). J Mol Graph Model. 2016. <https://doi.org/10.1016/j.jmgm.2016.03.015>.
- Ribeiro-Viana RM, Butera AP, Santos ES, Tischer CA, Alves RB, PereiraFreitas R, et al. Revealing the binding process of new 3-alkylpyridine marine alkaloid analogue antimalarials and the heme Group: an experimental and theoretical investigation. J Chem Inf Model. 2016. <https://doi.org/10.1021/acs.jcim.5b00742>.
- Barbosa CS, Guimarães DSM, Gonçalves AMMN, Barbosa MCS, Alves Costa ML, Nascimento Júnior CS, et al. Target-guided synthesis and antiplasmodial evaluation of a new fluorinated 3-alkylpyridine marine alkaloid analog. ACS Omega. 2017. <https://doi.org/10.1021/acsomega.7b01302>.
- Guimarães DSM, da Fonseca AL, Batista R, Comar Junior M, de Oliveira AB, Taranto AG, et al. Structure-based drug design studies of the interactions of ent-kaurene diterpenes derived from *Wedelia paludosa* with the *Plasmodium falciparum* sarco/endoplasmic reticulum Ca²⁺-ATPase PfATP6. Mem Inst Oswaldo Cruz. 2015. <https://doi.org/10.1590/0074-02760140415>.
- Nagasundaram N, Doss GPC, Chakraborty C, Karthick V, Kumar DT, Balaji V, Siva R, Luzz A, Gea Z, Zhuzhux H. Mechanism of artemisinin resistance for malaria PfATP6 L263 mutations and discovering potential antimalarial: an integrated computational approach. Sci Rep. 2016. <https://doi.org/10.1038/srep30106>.
- Xu X, Huang M, Zou X. Docking-based inverse virtual screening: methods, applications, and challenges. Biophys Reports. 2018. <https://doi.org/10.1007/s41048-017-0045-8>.
- Forli S, Huey R, Pique ME, Sanner MF, Goodsell DS, Olson AJ. Computational protein–ligand docking and virtual drug screening with the AutoDock suite. Nat Protoc. 2016. <https://doi.org/10.1038/nprot.2016.051>.
- Kim Bo-K, HyojinKo E-SJ, Eun-SeonJu LS, Jeong YCK. 2,3,4-Trihydroxybenzyl-hydrazone analogues as novel potent coxsackievirus B3 3C protease inhibitors. Eur J Med Chem. 2016. <https://doi.org/10.1016/j.ejmech.2016.03.085>.

35. Leigh M, Raines DJ, Castillo CE, Duhme-Klair AK. Inhibition of Xanthine Oxidase by thiosemicarbazones, hydrazones and dithiocarbazates derived from hydroxy-substituted benzaldehydes. *ChemMedChem*. 2011. <https://doi.org/10.1002/cmdc.201100054>.
36. Dai C-H, Mao F-L. N'-(3-Hidroxibenzilideno)-4-nitrobenzohidrazida. *Acta Crystallographica Seção E: Relatórios de Estrutura Online*. 2010. <https://doi.org/10.1107/S1600536811051233>.
37. Dutra LA, Frade J, Johmann N, Pires ME, Chin CM, Santos JL. Synthesis, antiplatelet and antithrombotic activities of resveratrol derivatives with NO-donor properties. *Bioorg Med Chem Lett*. 2017. <https://doi.org/10.1016/j.bmcl.2017.04.007>.
38. Zafar H, Hayat M, Saied S, Khan M, Salar U, Malik R, Khan KM. Xanthine oxidase inhibitory activity of nicotino/isonicotinohydrazides: a systematic approach from *in vitro*, *in silico* to *in vivo* studies. *Bioorg Med Chem*. 2017. <https://doi.org/10.1016/j.bmc.2017.02.044>.
39. Krake SH, Martinez PDG, McLaren J, Ryan E, Chen G, White K, et al. Novel inhibitors of *Plasmodium falciparum* based on 2,5-disubstituted furans. *Eur J Med Chem*. 2017. <https://doi.org/10.1016/j.ejmech.2016.12.024>.
40. Thota S, Rodrigues DA, Pinheiro PSM, Lima LM, Fraga CAM, Barreiro EJ. N-Acylhydrazones as drugs. *Bioorg Med Chem Lett*. 2018. <https://doi.org/10.1016/j.bmcl.2018.07.015>.
41. Amaral DN, Cavalcanti BC, Bezerra DP, Ferreira PMP, Castro RP, Sabino JR, et al. Docking, synthesis and antiproliferative activity of *n*-acylhydrazone derivatives designed as combretastatin A4 analogues. *PLoS ONE*. 2014. <https://doi.org/10.1371/journal.pone.0085380>.
42. Aarjane M, Aouidate A, Slassi S, Amine A. Synthesis, antibacterial evaluation, *in silico* ADMET and molecular docking studies of new N-acylhydrazone derivatives from acridone. *Arab J Chem*. 2020. <https://doi.org/10.1016/j.arabjch.2020.05.034>.
43. Romeiro NC, Aguirre G, Hernández P, González M, Cerecetto H, Aldana I, et al. Synthesis, trypanocidal activity and docking studies of novel quinoxaline-N acylhydrazones, designed as cruzain inhibitors candidates. *Bioorg Med Chem*. 2009. <https://doi.org/10.1016/j.bmc.2008.11.065>.
44. Inam A, Siddiqui SM, Macedo TS, Moreira DRM, Leite ACL, Soares MBP, et al. Design, synthesis and biological evaluation of 3-[4-(7-chloroquinolin-4-yl)-piperazin-1-yl]-propionic acid hydrazones as antiprotozoal agents. *Eur J Med Chem*. 2014. <https://doi.org/10.1016/j.ejmech.2014.01.023>.
45. Katsuno K, Burrows JN, Duncan K, Van Huijsduijnen RH, Kaneko T, Kita K, et al. Hit and lead criteria in drug discovery for infectious diseases of the developing world. *Nat Rev Drug Discov*. 2015. <https://doi.org/10.1038/nrd4683>.
46. Sijwali PS, Kato K, Seydel KB, Gut J, Lehman J, Klemba M, et al. *Plasmodium falciparum* cysteine protease falcipain-1 is not essential in erythrocytic stage malaria parasites. *Proc Natl Acad Sci USA*. 2004. <https://doi.org/10.1073/pnas.0402738101>.
47. Kerr ID, Lee JH, Pandey KC, Harrison A, Sajid M, Rosenthal PJ, et al. Structures of falcipain-2 and falcipain-3 bound to small molecule inhibitors: Implications for substrate specificity. *J Med Chem*. 2009. <https://doi.org/10.1021/jm8013663>.
48. Perozzo R, Kuo M, Sidhu ABS, Valiyaveetil JT, Bittman R, Jacobs WR, et al. Structural elucidation of the specificity of the antibacterial agent triclosan for malarial acyl carrier protein reductase. *J Biol Chem*. 2002. <https://doi.org/10.1074/jbc.M112000200>.
49. Parthasarathy S, Eazhisai K, Balaran H, Balaran P, Murthy MRN. Structure of *Plasmodium falciparum* Triose-phosphate Isomerase-2-Phosphoglycerate Complex at 1.1-Å Resolution. *J Biol Chem*. 2003. <https://doi.org/10.1074/jbc.M308525200>.
50. Peterson MR, Hall DR, Berriman M, Nunes JA, Leonard GA, Fairlamb AH, et al. The three-dimensional structure of a *Plasmodium falciparum* cyclophilin in complex with the potent anti-malarial cyclosporin A. *J Mol Biol*. 2000. <https://doi.org/10.1006/JMBI.2000.3633>.
51. Merckx A, Echaliar A, Langford K, Sicard A, Langsley G, Joore J, et al. Structures of *P. falciparum* protein kinase 7 identify an activation motif and leads for inhibitor design. *Structure*. 2008. <https://doi.org/10.1016/j.str.2007.11.014>.
52. Wrenger C, Müller IB, Schifferdecker AJ, Jain R, Jordanova R, Groves MR. Specific inhibition of the aspartate aminotransferase of *Plasmodium falciparum*. *J Mol Biol*. 2011. <https://doi.org/10.1016/j.jmb.2010.11.018>.
53. Hampton SE, Baragaña B, Schipani A, Bosch-Navarrete C, Musso-Buendía JA, Recio E, et al. Design, synthesis, and evaluation of 5'-diphenyl nucleoside analogues as inhibitors of the *Plasmodium falciparum* dUT-Pase. *ChemMedChem*. 2011. <https://doi.org/10.1002/cmdc.201100255>.
54. Boumis G, Giardina G, Angelucci F, Bellelli A, Brunori M, Dimastrogiovanni D, et al. Crystal structure of *Plasmodium falciparum* thioredoxin reductase, a validated drug target. *Biochem Biophys Res Commun*. 2012. <https://doi.org/10.1016/j.bbrc.2012.07.156>.
55. O'Rourke PE, Kalinowska-Tluścik J, Fyfe PK, Dawson A, Hunter WN. Crystal structures of IspF from *Plasmodium falciparum* and Burkholderia cenocepacia: comparisons inform antimicrobial drug target assessment. *BMC Struct Biol*. 2014. <https://doi.org/10.1186/1472-6807-14-1>.
56. Kasozi D, Mohring F, Rahlfs S, Meyer AJ, Becker K. Real-time imaging of the intracellular glutathione redox potential in the malaria parasite *Plasmodium falciparum*. *PLoS Pathog*. 2013. <https://doi.org/10.1371/journal.ppat.1003782>.
57. Pantouris G, Rajasekaran D, Garcia AB, Ruiz VG, Leng L, Jorgensen WL, et al. Crystallographic and receptor binding characterization of *Plasmodium falciparum* macrophage migration inhibitory factor complexed to two potent inhibitors. *J Med Chem*. 2014. <https://doi.org/10.1021/jm501168q>.
58. Silva AM, Lee AY, Gulnik SV, Majer P, Collins J, Bhat TN, et al. Structure and inhibition of plasmepsin II, a hemoglobin-degrading enzyme from *Plasmodium falciparum*. *Proc Natl Acad Sci USA*. 1996. <https://doi.org/10.1073/pnas.93.19.10034>.
59. Arnou B, Montigny C, Morth JP, Nissen P, Jaxel C, Møller JV, et al. The *Plasmodium falciparum* Ca²⁺-ATPase PfATP6: Insensitive to artemisinin, but a potential drug target. *Biochem Society Trans*. 2011. <https://doi.org/10.1042/BST0390823>.
60. Csermely P, Agoston V, Pongor S. The efficiency of multi-target drugs: the network approach might help drug design. *Trends Pharmacol Sci*. 2005. <https://doi.org/10.1016/j.tips.2005.02.007>.
61. Ritchie TJ, Macdonald SJ. The impact of aromatic ring count on compound developability—are too many aromatic rings a liability in drug design? *Drug Discov Today*. 2009. <https://doi.org/10.1016/j.drudis.2009.07.014>.
62. Ward SE, Beswick P. What does the aromatic ring number mean for drug design? *Expert Opin Drug Discov*. 2014. <https://doi.org/10.1517/17460441.2014.932346>.
63. Madrid DC, Ting L-M, Waller KL, Schramm VL, Kim K. *Plasmodium falciparum* purine nucleoside phosphorylase is critical for viability of malaria parasites. *J Biol Chem*. 2008. <https://doi.org/10.1074/jbc.M807218200>.
64. Schnick C, Robien MA, Brzozowski AM, Dodson EJ, Murshudov GN, Anderson L, et al. Structures of *Plasmodium falciparum* purine nucleoside phosphorylase complexed with sulfate and its natural substrate inosine. *Acta Crystallogr Sect D Biol Crystallogr*. 2005. <https://doi.org/10.1107/S0907444905020251>.
65. Gelpi J, Hospital A, Goñi R, Orozco M. Molecular dynamics simulations: advances and applications. *Adv Appl Bioinforma Chem*. 2015. <https://doi.org/10.2147/AABC.S70333>.
66. Freire AC, Podczek F, Sousa J, Veiga F. Liberação específica de fármacos para administração no cólon por via oral. I - O cólon como local de liberação de fármacos. *Rev Bras Ciências Farm*. 2006. <https://doi.org/10.1590/S1516-93322006000300003>.
67. de Souza J, Freitas ZMF, Storpirtis S. Modelos *in vitro* para determinação da absorção de fármacos e previsão da relação dissolução/absorção. *Rev Bras Ciências Farm*. 2017. <https://doi.org/10.1590/S1516-9332200700400004>.
68. Ndombera F, Maiyoh G, Tuei V. Pharmacokinetic, physicochemical and medicinal properties of n-glycoside anti-cancer agent more potent than 2-deoxy-dglucose in lung cancer cells. *J Pharmacy Pharmacol*. 2019. <https://doi.org/10.17265/2328-2150/2019.04.003>.
69. Lipinski CA, Lombardo F, Dominy BW, Feeney PJ. Experimental and computational approaches to estimate solubility and permeability in drug discovery and development settings. *Rev de Entrega de Medicamentos Adv*. 1997. [https://doi.org/10.1016/s0169-409x\(00\)00129-0](https://doi.org/10.1016/s0169-409x(00)00129-0).
70. Mishra S, Dahima R. *In vitro* ADME studies of TUG-891, a GPR-120 inhibitor using SWISS ADME predictor. *J Delivery Therap*. 2019. <https://doi.org/10.22270/jddt.v9i2-s.2710>.
71. Difa CA, Eze CK, Iyaji RF, Cosmas S, Durojaye AO. In-Silico pharmacokinetics study on the inhibitory potentials of the C=O derivative of gedunin and pyrimethamine against the *Plasmodium falciparum* dihydrofolate reductase. *Ciência*. 2018;4:137–42.

72. Ranjuth D, Ravikumar C. SwissADME predictions of pharmacokinetics and druglikeness properties of small molecules present in Ipomoea mauritiana Jacq. J Pharmacognosy Phytochemis. 2019;5:2063–73.
73. Bojarska J, Remko M, Breza M, Madura ID, Kaczmarek K, Zabrocki J, Wolf WM. A supramolecular approach to structure-based design with a focus on synthons hierarchy in ornithine-derived ligands: review, synthesis experimental in silico Studies. Molecules. 2020. <https://doi.org/10.3390/molecules25051135>.
74. Guilherme FD, Simonetti JÉ, Folquito LRS, Reis ACC, Oliver JC, Dias ALT, et al. Synthesis, chemical characterization and antimicrobial activity of new acylhydrazones derived from carbohydrates. J Mol Struct. 2019;1184:349–56.
75. Nugraha RYB, Faratisha IFD, Mardhiyyah K, Ariel DG, Putri FF, Nafisatuz-zamrudah SW, et al. Antimalarial properties of isoquinoline derivative from Streptomyces Hygroscopicus subsp. hygroscopicus: an in silico Approach. Biomed Res Int. 2020. <https://doi.org/10.1155/2020/6135696>.
76. Trager W, Jensen J. Human malaria parasites in continuous culture. Science. 1976. <https://doi.org/10.1126/science.781840>.
77. Lambros C, Vanderberg JP. Synchronization of *Plasmodium falciparum* erythrocytic stages in culture. J Parasitol. 1979;65:418–20.
78. Rieckmann KH, Campbell GH, Sax LJ, Ema JE. Drug sensitivity of *Plasmodium falciparum*. An in-vitro microtechnique. Lancet. 1978. [https://doi.org/10.1016/s0140-6736\(78\)90365-3](https://doi.org/10.1016/s0140-6736(78)90365-3).
79. Carmichael J, DeGraff WG, Gazdar AF, Minna JD, Mitchell JB. Evaluation of a tetrazolium-based semiautomated colorimetric assay: assessment of radiosensitivity. Cancer Res. 1987;47:943–6.
80. ChemAxon. ChemAxon - Software Solutions and Services for Chemistry and Biology. MarvinSketch, Version 16.10.31. 2016.
81. Elokely KM, Doerksen RJ. Docking challenge: protein sampling and molecular docking performance. J Chem Inf Model. 2013. <https://doi.org/10.1021/ci400040d>.
82. Stewart JJP. Optimization of parameters for semiempirical methods VI: more modifications to the NDDO approximations and re-optimization of parameters. J Mol Model. 2013. <https://doi.org/10.1007/s00894-012-1667-x>.
83. Stewart JJP. MOPAC: a semiempirical molecular orbital program. J Comput Aided Mol Des. 1990. <https://doi.org/10.1007/BF00128336>.
84. Gasteiger J, Marsili M. Iterative partial equalization of orbital electronegativity a rapid access to atomic charges. Tetrahedron. 1980. [https://doi.org/10.1016/0040-4020\(80\)80168-2](https://doi.org/10.1016/0040-4020(80)80168-2).
85. Morris GM, Huey R, Lindstrom W, Sanner MF, Belew RK, Goodsell DS, et al. AutoDock4 and AutoDockTools4: automated docking with selective receptor flexibility. J Comput Chem. 2009. <https://doi.org/10.1002/jcc.21256>.
86. Studio D. Dassault Systemes BIOVIA, Discovery Studio Modelling Environment, Release 4.5. Accelrys Softw Inc. 2015.
87. Trott O, Olson AJ. AutoDock Vina: Improving the speed and accuracy of docking with a new scoring function, efficient optimization, and multi-threading. J Comput Chem. 2009. <https://doi.org/10.1002/jcc.21334>.
88. Maia EHB, Campos VA, dos Reis SB, Costa MS, Lima IG, Greco SJ, et al. Octopus: a platform for the virtual high-throughput screening of a pool of compounds against a set of molecular targets. J Mol Model. 2017. <https://doi.org/10.1007/s00894-016-3184-9>.
89. Asojo OA, Gulnik SV, Afonina E, Yu B, Ellman JA, Haque TS, et al. Novel uncomplexed and complexed structures of plasmepsin II, an aspartic protease from *Plasmodium falciparum*. J Mol Biol. 2003. [https://doi.org/10.1016/s0022-2836\(03\)00036-6](https://doi.org/10.1016/s0022-2836(03)00036-6).
90. Clemente JC, Govindasamy L, Madabushi A, Fisher SZ, Moose RE, Yowell CA, et al. Structure of the aspartic protease plasmepsin 4 from the malarial parasite *Plasmodium malariae* bound to an allophenylborstatine-based inhibitor. Acta Crystallogr Sect D Biol Crystallogr. 2006. <https://doi.org/10.1107/S0907444905041260>.
91. Kerr ID, Lee JH, Pandey KC, Harrison A, Sajid M, Rosenthal PJ, et al. Structures of falcipain-2 and falcipain-3 bound to small molecule inhibitors: implications for substrate specificity. J Med Chem. 2009;52(3):852–7. <https://doi.org/10.1021/jm8013663>.
92. Bhaumik P, Xiao H, Parr CL, Kiso Y, Gustchina A, Yada RY, et al. Crystal Structures of the Histo-Aspartic Protease (HAP) from *Plasmodium falciparum*. J Mol Biol. 2009. <https://doi.org/10.1016/j.jmb.2009.03.011>.
93. Bhaumik P, Horimoto Y, Xiao H, Miura T, Hidaka K, Kiso Y, et al. Crystal structures of the free and inhibited forms of plasmepsin I (PMI) from

Plasmodium falciparum. J Struct Biol. 2011. <https://doi.org/10.1016/j.jsb.2011.04.009>.

Publisher's Note

Springer Nature remains neutral with regard to jurisdictional claims in published maps and institutional affiliations.

Ready to submit your research? Choose BMC and benefit from:

- fast, convenient online submission
- thorough peer review by experienced researchers in your field
- rapid publication on acceptance
- support for research data, including large and complex data types
- gold Open Access which fosters wider collaboration and increased citations
- maximum visibility for your research: over 100M website views per year

At BMC, research is always in progress.

Learn more biomedcentral.com/submissions

